Supporting Information

Buer et al. 10.1073/pnas.1120112109

SI Methods

Materials and Peptide Synthesis. L-5,5,5,5′,5′,5′-hexafluoroleucine was synthesized as described previously (1) and converted to Boc-protected derivative by standard procedures. 4,4,4-Trifluoroethylglycine was purchased from SynQuest Laboratory and enzymatically resolved as described previously (2). Peptides were synthesized by manual Fmoc procedures (α_4H) or manual Boc procedures (α_4F_3a and $\alpha_4F_3af_3d$) as described previously (3–5). All peptides were purified by preparatory RP-HPLC using a linear water to acetonitrile gradient containing 0.1% TFA. Peptide identity was confirmed using MALDI-MS with a matrix of α-cyano-4-hydroxycinnamic acid.

Crystallization. Peptides were dissolved in 10 mM Tris buffer (pH 7.0) to a concentration of 6 mM as determined by absorbance at 280 nm. Crystals were grown by vapor diffusion at 20 °C in a hanging drop with 2 μL peptide and 2 μL precipitant containing 100 mM CHES (N-cyclohexyl-2-aminoethanesulfonic acid) buffer (pH 9.0) and 48% (wt/vol) PEG 400 for α_4H, 100 mM Tris buffer (pH 7.8) and 55% (wt/vol) PEG 400 for α_4F_3a, and 100 mM Tris buffer (pH 8.5) and 48% (wt/vol) PEG 600 for $\alpha_4F_3af_3d$. Crystals were frozen with liquid N_2 in their mother liquor for data collection.

Data Collection and Refinement. Data were collected at the Advanced Photon Source (LS-CAT Beamlines 21-F and 21-G) at the Argonne National Laboratory and were collected on a MarCCD (Mar USA) at wavelengths of 0.97872 and 0.97857 Å, respectively, at −180 °C. Data were processed and scaled with HKL2000 (6). The peptides α_4H and α_4F_3a are crystallized in space group $I4_1$, with α_4H unit cell parameters of $a = b = 49.04$ Å, $c = 41.23$ Å, and $\alpha = \beta = \gamma = 90°$ and α_4F_3a unit cell parameters of $a = b = 48.35$ Å, $c = 39.75$ Å, and $\alpha = \beta = \gamma = 90°$. The peptide $\alpha_4F_3af_3d$ is in the space group $P2_12_12$ with unit cell parameters $a = 30.96$ Å, $b = 36.36$ Å, $c = 41.46$ Å, and $\alpha = \beta = \gamma = 90°$. All crystals contain a dimer in the asymmetric unit.

Phases were initially determined by molecular replacement using Phaser in the CCP4i suite of programs (7). The search model for α_4H was a helical monomer of 27 alanine residues based on the antiparallel structure of the four-helix bundle E20S (PDB ID code 2CCF) (8) built in Coot. For α_4F_3a and $\alpha_4F_3af_3d$, a monomer of α_4H was used as a starting model, with leucine (Leu) -10, -17, and -24 mutated to hexafluoroleucine and all other side chains truncated to Ala. The sequence register of the structures was determined using ARP/wARP (9). The PRODRG web server was used to generate coordinates and restraint parameters for hexafluoroleucine, trifluoroethylglycine, and non-water-solvent molecules (10). Peptide models were refined by rigid body refinement and restrained refinement using Buster (11). Side chains were built using Coot (12) with $2F_o - F_c$ and $F_o - F_c$ electron density maps from Buster. The refinement of α_4H to 1.36 Å resulted in $R_{work} = 19.7\%$ and $R_{free} = 25.5\%$. The refinement of α_4F_3a to 1.54 Å resulted in $R_{work} = 18.6\%$ and $R_{free} = 20.9\%$. The refinement of $\alpha_4F_3af_3d$ to 1.72 Å resulted in $R_{work} = 24.1\%$ and $R_{free} = 29.0\%$. All residues from the three structures are in the allowed regions of the Ramanchandran plot. Structures were validated with Molprobity (13), Parvarti (14), and whatcheck (15). Areas of poor electron density were not modeled. These areas include α_4H residue 27 of chain A and 1 and 27 of chain B, α_4F_3a residues 26 and 27 of chain A and 27 of chain B, and $\alpha_4F_3af_3d$ residues 1–4 and 27 of chain A and 26 and 27 of chain B. Data refinement and statistics are given in Table S1.

Structure Analysis. Protein models were generated, and hydrogens were added using Pymol. Protein volumes and surface areas were analyzed using MSMS (16) in Chimera with a probe radius of 1.4 Å corresponding to a water molecule and a vertex density of 10. The packing arrangement of the hydrophobic core of α_4H was analyzed by SOCKET (17).

Circular Dichroism. Circular dichroism spectra of peptides were recorded with an Aviv 62DS spectropolarimeter at 25 °C. To examine the unfolding of the peptide by GuHCl, stock solutions were prepared containing 40 μM peptide (concentration of monomer) in 10 mM potassium phosphate buffer, pH 7.0, both with and without 8.0 M GuHCl. An autotitrator was used to mix the two solutions to incrementally increase the concentration of GuHCl in the sample circular dichroism cuvettete (path length = 1 cm); after equilibration, the ellipticity at 222 nm was measured. The denaturation curves for each peptide are shown in Fig. S4.

Curve Fitting. The denaturation profiles for the peptides were analyzed assuming a two-state equilibrium between unfolded monomeric peptide and folded tetrameric bundle and assuming no significantly populated intermediates present, which was described previously (4). Igor Pro software (Wavemetrics, Inc.) was used to fit the denaturation curves. Robust fits were obtained for each peptide, which is shown in Fig. S4. For $\alpha_4F_3af_3d$, the absence of a lower baseline limited the accuracy with which ΔG_{fold} could be determined, resulting in a larger error in this measurement than for the other two peptides.

1. Anderson JT, Toogood PL, Marsh ENG (2002) A short and efficient synthesis of L-5,5,5,5′,5′,5′-hexafluoroleucine from N-Cbz-L-serine. *Org Lett* 4:4281–4283.
2. Buer BC, Chugh J, Al-Hashimi HM, Marsh ENG (2010) Using fluorine nuclear magnetic resonance to probe the interaction of membrane-active peptides with the lipid bilayer. *Biochemistry* 49:5760–5765.
3. Lee H-Y, Lee K-H, Al-Hashimi HM, Marsh ENG (2006) Modulating protein structure with fluorous amino acids: Increased stability and native-like structure conferred on a 4-helix bundle protein by hexafluoroleucine. *J Am Chem Soc* 128:337–343.
4. Lee K-H, Lee H-Y, Slutsky MM, Anderson JT, Marsh ENG (2004) Fluorous effect in proteins: de novo design and characterization of a four-α-helix bundle protein containing hexafluoroleucine. *Biochemistry* 43:16277–16284.
5. Buer BC, de la Salud-Bea R, Al Hashimi HM, Marsh ENG (2009) Engineering protein stability and specificity using fluorous amino acids: The importance of packing effects. *Biochemistry* 48:10810–10817.
6. Otwinowski Z, Minor W (1997) Processing of X-ray diffraction data collected in oscillation mode. *Methods Enzymol* 276:307–326.
7. McCoy AJ, et al. (2007) Phaser crystallographic software. *J Appl Cryst* 40:658–674.
8. Yadav MK, et al. (2006) Coiled coils at the edge of configurational heterogeneity. Structural analyses of parallel and antiparallel homotetrameric coiled coils reveal configurational sensitivity to a single solvent-exposed amino acid substitution. *Biochemistry* 45:4463–4473.
9. Langer G, Cohen SX, Lamzin VS, Perrakis A (2008) Automated macromolecular model building for X-ray crystallography using ARP/wARP version 7. *Nat Protoc* 3:1171–1179.
10. Schüttelkopf AW, van Aalten DMF (2004) PRODRG: A tool for high-throughput crystallography of protein-ligand complexes. *Acta Crystallogr D Biol Crystallogr* 60:1355–1363.
11. Bricogne G, et al. (2011) *BUSTER Version 1.6.0* (Global Phasing Ltd., Cambridge, UK).
12. Emsley P, Cowtan K (2004) Coot: Model-building tools for molecular graphics. *Acta Crystallogr D Biol Crystallogr* 60:2126–2132.
13. Davis IW, et al. (2007) MolProbity: All-atom contacts and structure validation for proteins and nucleic acids. *Nucleic Acids Res* 35:W375–W383.
14. Zucker F, Champ PC, Merritt EA (2010) Validation of crystallographic models containing TLS or other descriptions of anisotropy. *Acta Crystallogr D Biol Crystallogr* 66:889–900.
15. Hooft RWW, Vriend G, Sander C, Abola EE (1996) Errors in protein structures. *Nature* 381:272.
16. Sanner MF, Olson AJ, Spehner J-C (1996) Reduced surface: An efficient way to compute molecular surfaces. *Biopolymers* 38:305–320.
17. Walshaw J, Woolfson DN (2001) Socket: A program for identifying and analysing coiled-coil motifs within protein structures. *J Mol Biol* 307:1427–1450.

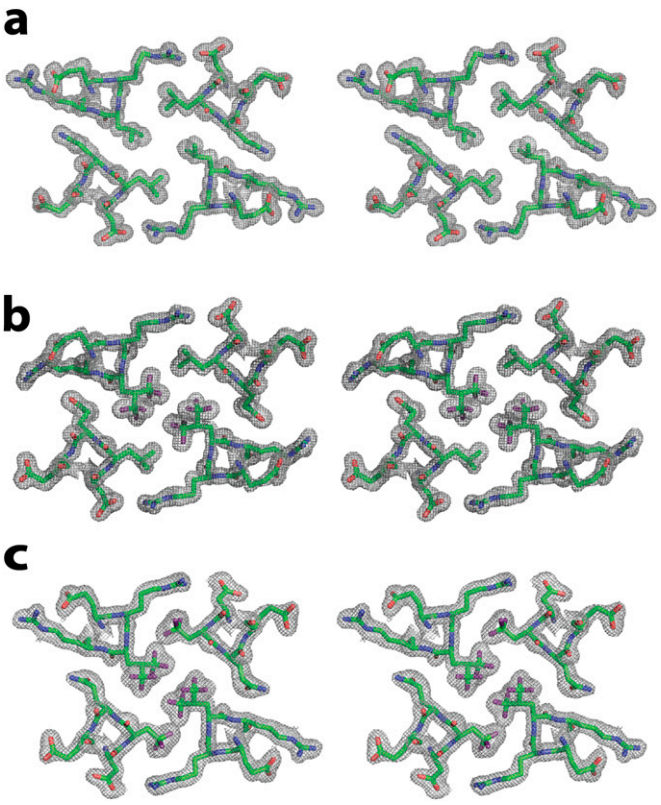

Fig. S1. Stereoviews of the electron density for layer 3 of α_4H, α_4F_3a, and $\alpha_4F_3af_3d$. (*A*) α_4H. (*B*) α_4F_3a. (*C*) $\alpha_4F_3af_3d$.

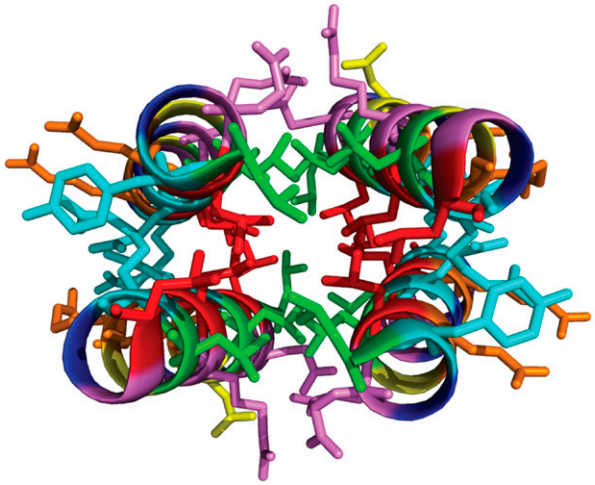

knob residue	side-chain packing angle (degrees)
LeuA10	64.15
LeuA13	132.92
LeuA17	58.08
LeuA20	137.82
LeuB10	73.90
LeuB13	135.50
LeuB17	57.56
LeuB20	131.11

Fig. S2. (*Left*) Structure of the coiled-coil region of α_4H. The colored helices were identified as coiled coils by SOCKET with knobs shown as sticks. Leu residues in the a and d positions of the heptad repeat are colored red and green, respectively. The default packing cutoff of 7 Å was used. (*Right*) Side chain packing angles of SOCKET identified type 4 knobs into holes-participating Leu residues. Residues in the a position have an average packing angle of 63.42°, whereas residues in the d position have an average packing angle of 134.34°. Angles were generated by SOCKET, which measures the C_α–C_β bond vector of the knob residue relative to the C_α–C_α bond vector of the two residues on the sides of the corresponding hole.

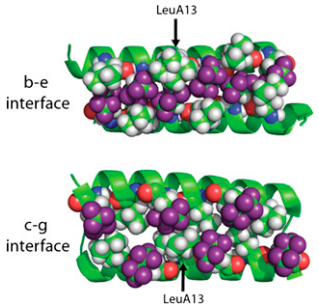

Fig. S3. Conformational mobility observed for LeuA13 in the structure of α_4F_3a. The electron density for this residue could be modeled in two slightly different conformations as shown, each with ~50% occupancy.

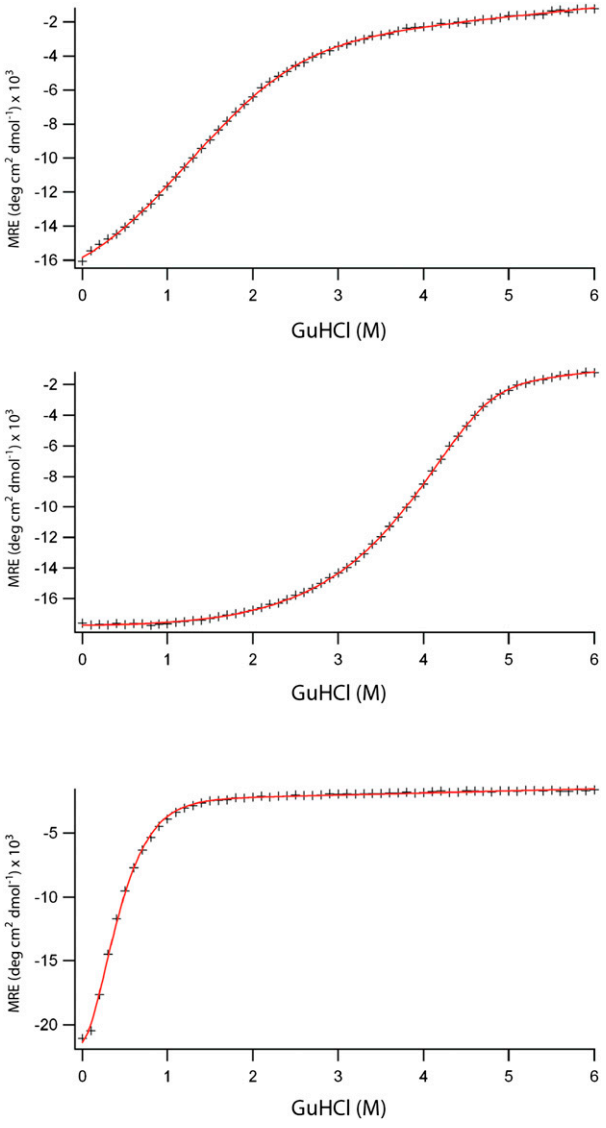

Fig. S4. Guanidine hydrochloride induced unfolding curves and fits for α_4H (*Top*), α_4F_3a (*Middle*), and $\alpha_4F_3af_3d$ (*Bottom*). Unfolding was monitored by following changes in ellipticity at 222 nm. Free energies of folding were calculated as described in the text.

Table S1. Data collection and refinement statistics

Dataset	α_4H	α_4F_3a	$\alpha_4F_3af_3d$
Space group	$I4_1$	$I4_1$	$P2_12_12$
Unit cell	$a = b = 49.04$; $c = 41.23$; $\alpha = \beta = \gamma = 90$	$a = b = 48.35$; $c = 39.75$;$\alpha = \beta = \gamma = 90$	$a = 30.96$; $b = 36.36$; $c = 41.46$; $\alpha = \beta = \gamma = 90$
Wavelength (Å)	0.97872	0.97872	0.97872
Resolution (Å)	1.36 (1.36–1.38)	1.54 (1.54–1.57)	1.72 (1.72–1.75)
R_{sym} (%)	4.7 (25.8)	5.3 (27.6)	4.6 (52.3)
{I/σI}	20 (5)	20 (5)	20 (3)
Completeness (%)	99.1 (99.6)	98.8 (100.0)	99.3 (100.0)
Redundancy	7.3 (6.6)	7.0 (6.5)	10.3 (10.7)
Refinement statistics			
Resolution (Å)	1.36 (10.0–1.36)	1.54 (34.19–1.54)	1.72 (9.08–1.72)
R factor (%)	19.7	18.6	24.1
R_{free} (%)	25.5	20.9	29.0
Protein atoms	439	457	459
Water molecules	41	19	19
Unique reflections	10,467	6,778	5,229
rmsd			
Bonds	0.010	0.009	0.009
Angles	0.96	1.05	1.17
MolProbity score	4.34	0.00	1.41
Clash score	1.21	0.50	0.87